

A Universal Scheme for Patterning of Oxides via Thermal Nanoimprint Lithography

Saman Safari Dinachali, Mohammad S. M. Saifullah,* Ramakrishnan Ganesan,*
Eng San Thian, and Chaobin He

To Professor Vikram Jayaram, for his contribution to ceramic engineering

Direct patterning of oxides using thermal nanoimprint lithography is performed using either the sol-gel or methacrylate route. The sol-gel method results in resists with long shelf-life, but with high surface energy and a considerable amount of solvent that affects the quality of imprinting. The methacrylate route, which is limited to certain oxides, produces polymerizable resists, leading to low surface energy, but suffers from the shorter shelf-life of precursors. By combining the benignant elements from both these routes, a universal method of direct thermal nanoimprinting of oxides is demonstrated using precursors produced by reacting an alkoxide with a polymerizable chelating agent such as 2-(methacryloyloxy)ethyl acetoacetate (MAEAA). MAEAA possesses β -ketoester, which results in the formation of environmentally stable, chelated alkoxide with long shelf-life, and methacrylate groups, which provide a reactive monomer pendant for in situ copolymerization with a cross-linker during imprinting. Polymerization leads to trapping of cations, lowering of surface energy, strengthening of imprints, which enables easy and clean demolding over 1 cm \times 2 cm patterned area with \approx 100% yield. Heat-treatment of imprints gives amorphous/crystalline oxide patterns. This alliance between two routes enables the successful imprinting of numerous oxides including Al_2O_3 , Ga_2O_3 , In_2O_3 , Y_2O_3 , B_2O_3 , TiO_2 , SnO_2 , ZrO_2 , GeO_2 , HfO_2 , Nb_2O_5 , Ta_2O_5 , V_2O_5 , and WO_3 .

1. Introduction

Due to its facile, cost-effective and high throughput production process, nanoimprint lithography (NIL) has garnered increasing attention as a next-generation patterning technique that allows the fabrication of structures from micro- to nanoscale at high resolution and precision with device applications in

optoelectronics, photonics, data storage, and biology.^[1–4] In comparison to traditional lithography techniques in which chemical and physical properties of resist materials are modified by photons or electrons, NIL utilizes mechanical deformation of a resist material using a mold containing surface relief features at a controlled temperature and pressure to achieve higher resolution. In 2005, the International Technology Roadmap for Semiconductors (ITRS) listed NIL as one of the contender technologies for future generation chip manufacturing.^[5]

Thermal NIL is the most versatile of all the imprint techniques. This technique began as a way to replicate mold patterns into a thermoplastic material by heating the polymer above its glass transition temperature and applying pressure on the mold. Variations of this technique extended its adaptability to utilize materials such as thermosets, sol-gel films, metal-organic materials and polymerizable liquid metal methacrylate resists to pattern organic as well as inorganic materials, especially oxides.^[6–18] Direct

NIL of oxides has generated tremendous interest due to the fact that their physical properties can be tailored by nanoscale patterning. One- or two-dimensional nanostructured oxides are expected to play an important role as functional units in electronic, optoelectronic and photonic devices.^[16] Since oxides are hard materials and do not have a workable softening point, they are imprinted using a “soft” and “moldable” precursors.

S. S. Dinachali, Dr. M. S. M. Saifullah, Prof. C. He
Institute of Materials Research and Engineering
A*STAR (Agency for Science, Technology and Research)
3 Research Link, Singapore 117602, Republic of Singapore
E-mail: saifullahm@imre.a-star.edu.sg

S. S. Dinachali, Dr. E. S. Thian
Department of Mechanical Engineering
National University of Singapore
9 Engineering Drive 1, Singapore 117576, Republic of Singapore

DOI: 10.1002/adfm.201202577

Dr. R. Ganesan
Department of Chemistry
Birla Institute of Technology & Science
Pilani–Hyderabad Campus,
Jawahar Nagar, Shameerpet Mandal,
Hyderabad–500 078, Andhra Pradesh, India
E-mail: ram.ganesan@bits-hyderabad.ac.in

Prof. C. He
Department of Materials Science & Engineering
National University of Singapore
21 Lower Kent Ridge Road, Singapore 119077, Republic of Singapore



The patterned precursor is then heat-treated to yield structured oxide. The two popular methods for direct patterning of oxides using NIL are the sol-gel and methacrylate routes. The sol-gel route with its low-temperature characteristics, good film quality, and as an economical way to obtain engineered ceramics has attracted a great deal of attention in the imprint technology. In this route, usually an alkoxide or acetate is used as an oxide precursor.^[6–15] If an alkoxide is used, it is stabilized against hydrolysis by a chelating agent, usually a β -diketone or β -ketoester, in an alcohol medium. The chelated alkoxide or acetate solution is spin-coated on a substrate and patterned using soft stamps such as polydimethylsiloxane (PDMS) and perfluoropolyether (PFPE) at a set pressure and temperature. However, direct imprinting of oxides via this route faces two major challenges. Firstly, due to high surface energy of the precursors, the sol-gel imprinting requires a good mold release system,^[6] and secondly, the solvent in sol-gel film, which helps to “softer” it for imprint process, may get trapped in the imprinted structures leading to incomplete filling of the precursor material inside the mold and resulting in poor demolding. Moreover, soft molds are amenable to deformation, especially when sub-100-nm features are desired. On the other hand, the methacrylate resists are prepared by reacting metal alkoxides with methacrylic acid. The reaction leads to the formation of liquid metal methacrylate, i.e., a clear solution of metal methacrylate in an alcohol byproduct. This polymerizable precursor is mixed with a cross-linker such as ethylene glycol dimethacrylate (EDMA) to form the resist for imprinting. In situ free-radical thermal copolymerization during imprinting leads to the reduction of surface energy and strengthening of patterned structures thereby giving yields close to 100%.^[17,18] Furthermore, this approach incorporates the benefits of a rigid silicon mold and liquid precursor to achieve very high resolution over areas $>1\text{ cm} \times 1\text{ cm}$ but at a lower temperature and imprinting pressure. However, this route has limited applicability due to the instability of many metal methacrylates.^[18]

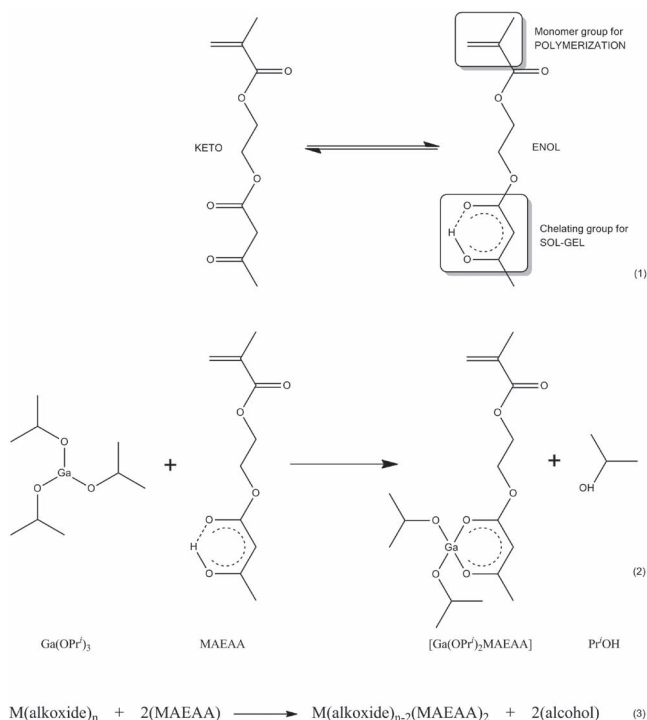
In this work, we show an alternative method and a universal route to the direct nanoimprint lithography of oxides by harnessing the advantages of the sol-gel and polymerizable liquid methacrylate resist routes and at the same time alleviate the disadvantages associated with both these methods. This synergy can be achieved when alkoxides are complexed with a polymerizable chelating agent such as 2-(methacryloyloxy)ethyl acetoacetate (MAEAA). MAEAA possesses β -ketoester and methacrylate groups, the former can lead to the formation of environmentally stable, chelated alkoxide complex while the latter provides the reactive methacrylate group for in situ copolymerization with a cross-linker during imprinting. Our preliminary work on imprinting of Al_2O_3 via this route has shown a considerable amount of promise.^[19] Using the synergistic effect of β -ketoester and methacrylate groups in the chelating monomer MAEAA, we demonstrate a universal scheme for direct thermal NIL of various oxides such as Al_2O_3 , Ga_2O_3 , In_2O_3 , Y_2O_3 , B_2O_3 , TiO_2 , SnO_2 , ZrO_2 , GeO_2 , HfO_2 , Nb_2O_5 , Ta_2O_5 , V_2O_5 , and WO_3 . Furthermore, our approach also incorporates the benefits of a rigid mold and liquid precursor to achieve very high resolution over areas $1\text{ cm} \times 2\text{ cm}$ but at a lower temperature and pressure to obtain yields of almost 100% after imprinting. For the sake of better understanding of the NIL process, our study

has divided patterning process based on the oxidation state of the above-mentioned cations, i.e., +3, +4, and +5 (and above). Although examples of imprinting of all the oxides will be given, only two cations from each category will be used as representative candidates for discussing the resist behaviour. They are Al and Ga for +3; Ti and Sn for +4; and Nb and Ta for +5 valencies and above.

2. Results and Discussion

Alkoxides are very reactive compounds due to the presence of electronegative alkoxy groups, which make the cations highly prone to nucleophilic attack. Due to their high affinity with water, hydrolysis results in the formation of molecular aggregates of hydrated alkoxides. However, the hydrolytic reactivity of alkoxides can be controlled by complexation/chelation with β -diketones, β -ketoesters, acetic acid among others.^[20] This chemical modification leads to the alteration of the whole hydrolysis-condensation process, enabling an easy and economic way to process sol-gel materials to obtain ceramics. However, an addition of extra pendant group to chelating agents such as β -diketones and β -ketoesters offers exciting possibilities to increase the latitude of ceramic processing. For example, ethylacetoacetate is a well-known β -ketoester for stabilizing alkoxides against hydrolysis by chelation for sol-gel processing.^[21] If a hydrogen atom from the ethyl group is replaced by a methacryloyloxy group, it leads to the formation of a bi-functional molecule which can not only chelate with alkoxides but also undergoes polymerization in the presence of a thermal free radical initiator.^[22] The latter is due to the fact that the methacrylate group in methacryloyloxy unit is a highly reactive polymerizable monomer. This is precisely what 2-(methacryloyloxy)ethyl acetoacetate (or MAEAA) does in the presence of an alkoxide. It chelates with an alkoxide to prevent its hydrolysis as well as provides the methacrylate group for polymerization. In other words, the chelated monomer-based precursor thus formed synergistically utilizes the advantages associated with both sol-gel and methacrylate chemistries, thereby leading to a much wider scope for processing of materials. Similar to other β -diketones and β -ketoesters, MAEAA is capable of keto-enol tautomerism, as shown in Equation 1. The enol form of MAEAA is stabilized by chelation with an alkoxide. Further, the reaction also results in the stoichiometric replacement of an alkoxy group (e.g., an *iso*-propoxy group from gallium (III) *iso*-propoxide) by a β -ketoester ligand,^[23–25] as shown in Equation 2. The general reaction of an alkoxide with MAEAA is shown in Equation 3. The hydrolytic activity of the stabilized alkoxide is substantially reduced, perhaps due to steric hindrance. This chelation reaction, often accompanied by a color change of the solution (Table 1), yields a clear, flowable and polymerizable oxide precursor.

The FTIR spectroscopy was used to characterize the reaction between alkoxides and MAEAA (Figure 1). The FTIR spectra of the chelated precursors are similar and show a large number of absorption bands/peaks between 750 and 1800 cm^{-1} (Table 2). The pair of absorption peaks close to 1609 cm^{-1} and 1522 cm^{-1} is attributed to the bidentate character of cation-bonded MAEAA and hence is indicative of the formation of the chelated



complex.^[24,25] These peaks correspond to the $\nu(\text{C}=\text{O})$ and $\nu(\text{C}=\text{C})$ vibrations of the chelate ring, respectively. More importantly, the MAEAA-functionalized oxide precursors also show characteristic peaks of carbonyl group at 1721 cm^{-1} , and methacrylate double bond at 1634 cm^{-1} , the latter clearly suggesting the preservation of polymerizable double bond in the complexes. A shoulder at 1746 cm^{-1} in the FTIR spectra that corresponds to

Table 1. Observation of color change due to the chelation reaction between alkoxides and MAEAA.

Alkoxide	Color/Appearance after the chelation reaction
aluminium (III) tri- <i>sec</i> -butoxide	faint yellow/clear
gallium (III) <i>iso</i> -propoxide	faint yellow/clear
indium (III) <i>iso</i> -propoxide	faint yellow/clear
yttrium (III) <i>n</i> -butoxide	faint yellow/clear
tri- <i>iso</i> -propyl borate	no color/clear
titanium (IV) <i>n</i> -butoxide	lemon yellow/clear
zirconium (IV) <i>n</i> -butoxide	light brown/clear
tin (IV) <i>tert</i> -butoxide	faint yellow/clear
germanium (IV) ethoxide	light brown/clear
hafnium (IV) <i>tert</i> -butoxide	brown/clear
niobium (V) ethoxide	no color/clear
tantalum (V) <i>n</i> -butoxide	no color/clear
vanadium (V) tri- <i>iso</i> -propoxide oxide	reddish brown/clear
tungsten (V) ethoxide	yellow/clear

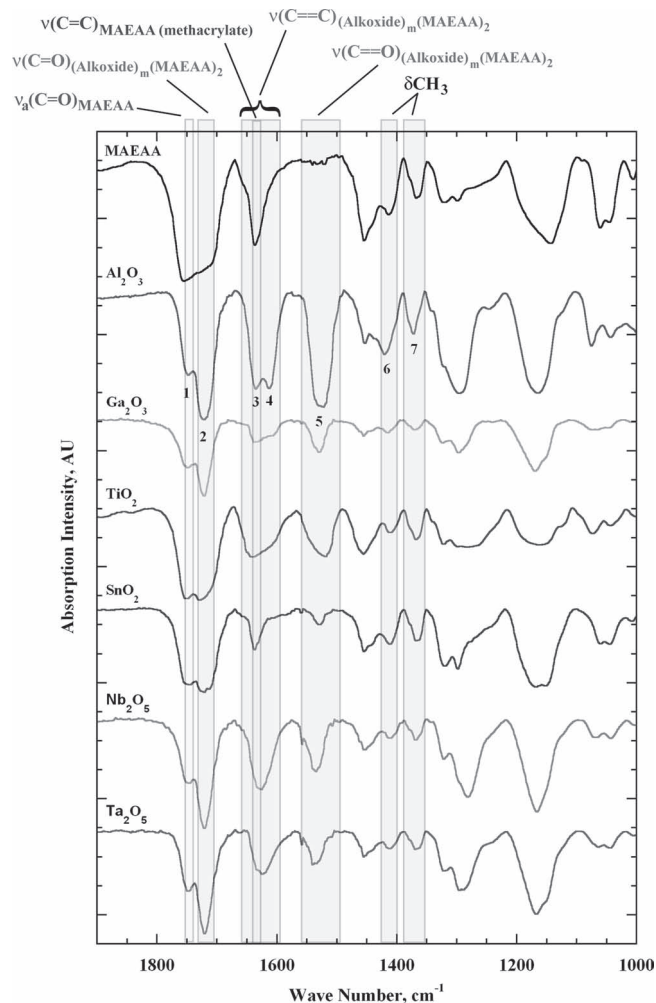


Figure 1. Characteristic infrared absorption peaks of oxide precursors formed by reacting alkoxide and MAEAA in a 1:2 ratio. The general formula of the precursor is $(\text{alkoxide})_m(\text{MAEAA})_2$. The broad vibration bands corresponding to particular bonds are indicated on top. Table 2 shows details of the band assignment.

the carbonyl group of MAEAA may indicate incomplete reaction between MAEAA and the corresponding alkoxides (Figure 1).^[25]

Stability of the chelate rings indicates the atmospheric stability of the chelated precursors. **Figure 2** shows the FTIR spectra of the representative precursors for each valency recorded at 0, 6 and 24 h under ambient laboratory conditions of $30\text{ }^\circ\text{C}$ and at $\approx 40\%$ relative humidity. It is seen that for all the precursors, even after 24 h, the FTIR spectra shows hardly any change in the peaks associated with the chelate rings. This shows that they are stable in normal laboratory conditions. Unsurprisingly, all the chelated precursors showed exceptional stability over a storage period of more than 3 months at room temperature. They were found to be clear and flowable.

Oxide resists for NIL were prepared by adding cross-linker EDMA and free-radical initiator benzoyl peroxide (BPO) to the corresponding chelated precursors. They were subjected to TGA and DSC studies in order to understand their degradation behaviour and to identify the polymerization exotherm, respectively

Table 2. Characteristic infrared absorption peaks of chelated oxide precursors. Albeit the principal peaks indicated below are for the Al_2O_3 precursor, other chelated precursors show similar values as seen in Figure 1.

Absorption peak [cm^{-1}]	Assignment	Peak number
1746	$\nu_a(\text{C}=\text{O})$	1
1721	$\nu(\text{C}=\text{O})$	2
1634	$\nu(\text{C}=\text{C})$	3
1609	$\nu(\text{C}=\text{O})$	4
1522	$\nu(\text{C}=\text{C})$	5
1418, 1372	δCH_3	6,7

(Figure 3). The TGA measurement in air showed a two-step mass loss. The minor loss from 30 °C to 150 °C was due to the loss of alcohol byproduct/solvent and the major loss from 300 °C to 550 °C occurred due to the degradation of organic component. Beyond 550 °C, a constant residual weight was observed due to

the formation of corresponding oxides (Figure 3a). The DSC scan showed that the thermal free radical copolymerization of chelated precursor and EDMA mixture in various resists occurred in a narrow range of temperatures, i.e., 80–130 °C (Figure 3b). For every oxide resist, their respective polymerization exotherm was used as a guide to initiate in situ free radical copolymerization during NIL. Time-resolved FTIR studies were also used to monitor the thermal copolymerization reaction in the oxide resists (Figure 4). The FTIR spectrum of the oxide resists before polymerization closely resembles their respective precursors. It was observed that after the thermal copolymerization, the intensity of the methacrylate double bond at 1634 cm^{-1} decreased significantly. It is noteworthy that the enolic $\nu(\text{C}=\text{O})$ at 1609 cm^{-1} and enolic $\nu(\text{C}=\text{C})$ complexed with cation at 1522 cm^{-1} remain unaffected after the polymerization. This confirms the fact that the cations remain trapped inside the polymer matrix after the polymerization reaction.

2.1. Nanoimprint Lithography of Oxides

The schematic of the steps involved in direct NIL of oxides is shown in Figure 5. Imprinting of all the oxide resists were carried out in two steps. Firstly, at room temperature (30 °C) a pressure of 30 bar was applied for 300 s to ensure a complete filling of the 250 nm equal line-and-space grating mold (aspect ratio 1) with the resist. Secondly, whilst holding the pressure constant, the coated substrate and mold were heated between 110 and 130 °C for 1000–1600 s in order to induce thermal free radical copolymerization in oxide resists. This leads to hardening of the imprint. The assembly was cooled down to room temperature after imprinting. The pressure was then released which was followed by a clean demolding, giving $\approx 100\%$ yield over $\approx 1 \text{ cm} \times 2 \text{ cm}$ area. Cross-sectional SEM studies show that the width and height of the imprinted features were slightly smaller than the actual dimensions of the mold, a result most likely due to the polymerization-induced shrinkage of the patterns.^[26]

The minimum temperature required to burn off the organic content completely from the oxide resists was determined using the isothermal TGA analysis. Table 3 provides the heat-treatment conditions used to convert imprinted resists to amorphous/crystalline oxide patterns. Ceteris paribus, the shrinkage of the imprints depends upon the metal atom, the size of the alkoxy group in precursor, heat-treatment temperature and the size of unit cell of metal oxide formed after heat-treatment. With some exceptions, generally speaking, pattern shrinkage close to 80% with respect to the original mold size was observed (Table 3). Except for WO_3 , in

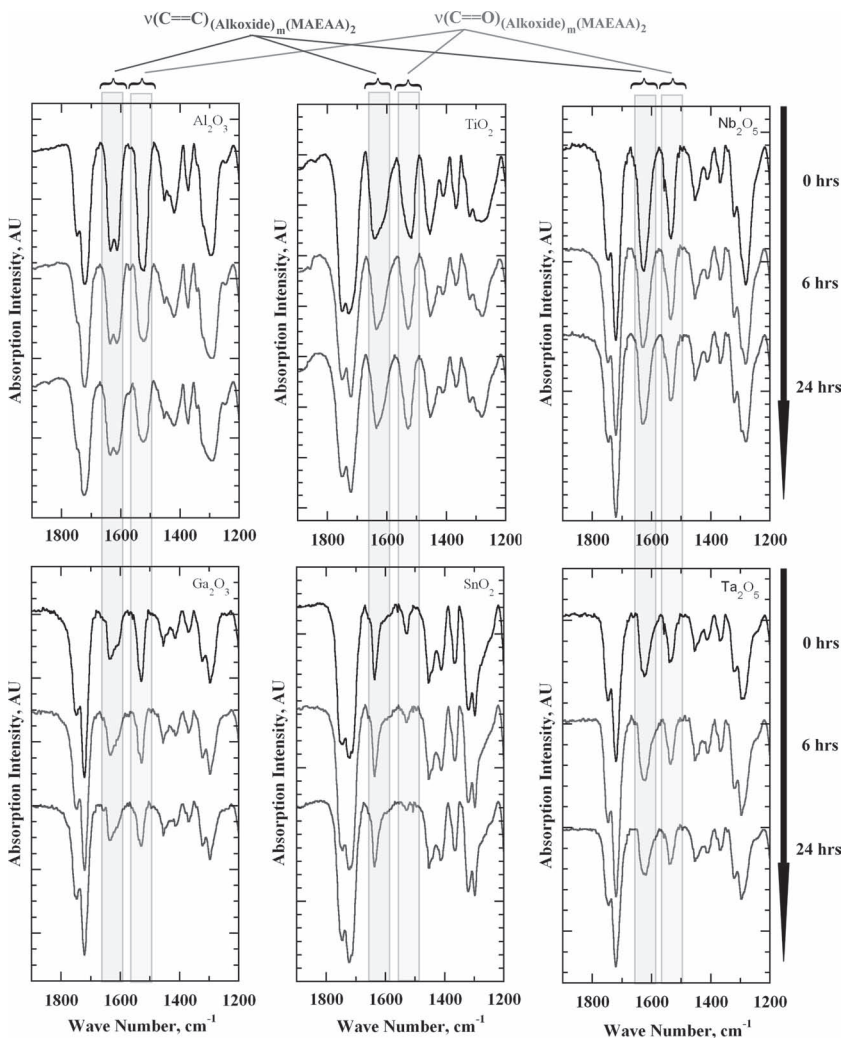


Figure 2. Atmospheric stability of as-coated precursor films, after 6 and 24 h at 30 °C and 40% relative humidity.

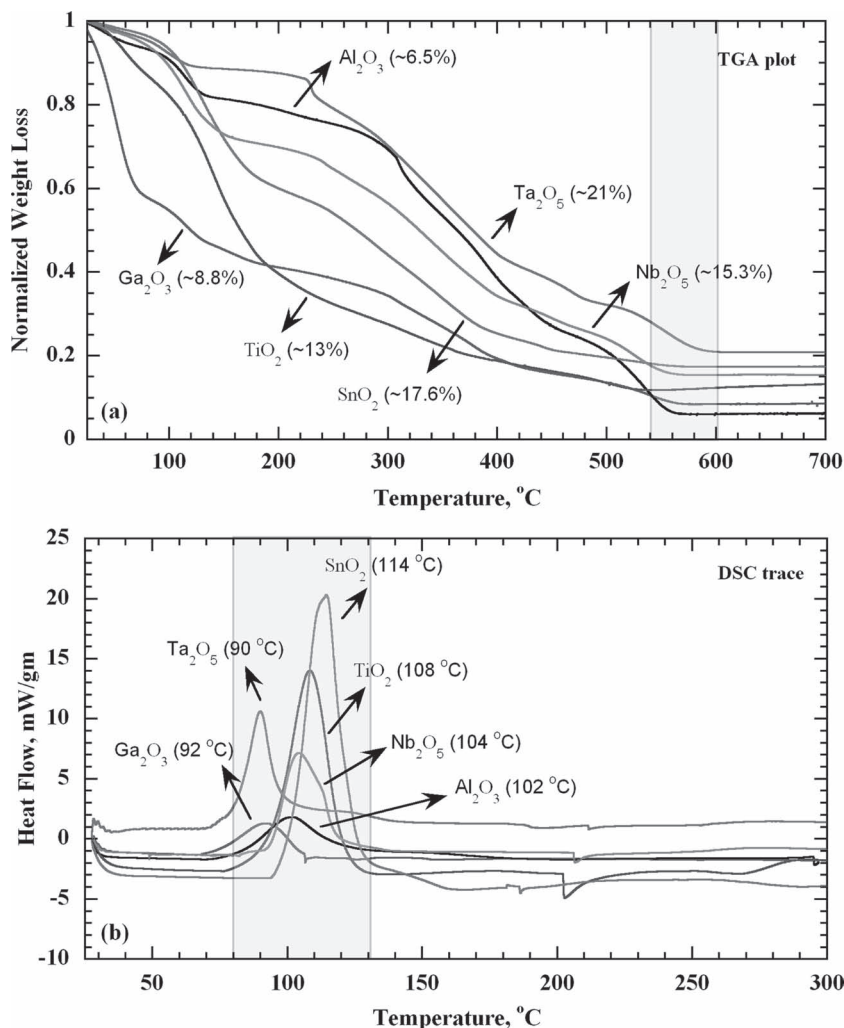


Figure 3. a) TGA analysis of the Al_2O_3 , Ga_2O_3 , TiO_2 , SnO_2 , Nb_2O_5 , and Ta_2O_5 resists showing mass losses during continuous heating to 800 °C. b) DSC data showing the exothermic peaks of onset of the thermal free-radical copolymerization in Al_2O_3 , Ga_2O_3 , TiO_2 , SnO_2 , Nb_2O_5 , and Ta_2O_5 resists.

all the cases, the imprinted structures maintain their integrity even after the heat-treatment. The AFM analysis showed that the aspect ratio between 0.5 and 1.5 (as opposed to the aspect ratio of 1 for molds used in the imprinting) was achieved for oxide patterns after heat treatment (Figures 6–8). The reason for such a difference of aspect ratios in various oxides may be primarily attributed to the difference in organic content before heat-treatment. However, the shrinkage appears to be nearly uniform over the entire imprinted structure. Although there is a reduction in the size of the patterns after heat-treatment, the center-to-center pattern distance remains the same whilst the edge-to-edge pattern distance increases, keeping the feature density of heat-treated patterns unchanged. While the calcination shrinkage comes at the cost of pattern size, it is actually an easy and cheaper way to access the nanoscale. As the aim is to minimize the organic losses and maximize the oxide content after heat-treatment in patterns without compromising their integrity, a judicious formulation of the composition of resist

containing alkoxide, MAEAA and EDMA is essential. In our case, their relative ratios were 1:2:1.5. The reason for choosing to react an alkoxide and MAEAA in a molar ratio of 1:2 for direct NIL of oxides is three-fold. Firstly, the presence of two reactive methacrylate groups chelated to the alkoxide atom provides better probability for them to get co-polymerized with the cross-linker, thereby trapping the cation inside the polymer network. Secondly, having more than two chelated MAEAA groups attached to the cation does not provide any additional benefit except to increase the undesirable mass loss during final heat-treatment to convert the imprinted structure to oxide. Thirdly, there is hardly any difference between the atmospheric stability of complexes which have one or three chelated MAEAA groups.^[19] On the other hand, the ratio of 2:1.5 between MAEAA and EDMA lead to consistently high yields close to $\approx 100\%$. This may be due to the increased degree of polymerization. Furthermore, this composition of resist also determines the imprinting time. The imprinting time can be significantly reduced if the amount of the EDMA is increased. However, a penalty is paid in the form of increased organic losses leading to smaller amount of remnant oxide after heat-treatment in the imprinted patterns.

Figure 6 shows the FE-SEM images of as-imprinted and heat-treated structures of Al_2O_3 , Ga_2O_3 , In_2O_3 , Y_2O_3 and B_2O_3 patterned using their respective resists containing +3 valency cations. None of these resists were found to be imprintable using the methacrylate route.^[18] However, the sol-gel route appears to be successful in patterning Al_2O_3 and In_2O_3 —the former used the nitrate route^[8] whilst the latter was imprinted

using a commercially available sol-gel-based indium-tin oxide precursor.^[12] Out of these resists, the most interesting case is that of B_2O_3 . The precursor for B_2O_3 resist was prepared by reacting tri-*iso*-propyl borate with MAEAA in a 1:2 molar ratio. However, the FTIR study of the precursor indicates that there is hardly any chelation between the alkoxide and MAEAA (see Supporting Information). This is not surprising as tri-*iso*-propyl borate is well-known for its inability to chelate under normal conditions.^[27] However, the presence of MAEAA and cross-linker EDMA in B_2O_3 resist resulted in in situ copolymerization during imprinting leading to the trapping of tri-*iso*-propyl borate in the polymer structure. This clearly suggests that alkoxides such as tetraethoxysilane (a precursor for SiO_2), which do not chelate easily with β -ketoesters, may also be imprinted using this method.

TiO_2 , ZrO_2 , SnO_2 , GeO_2 and HfO_2 resists containing +4 valency cations were imprinted and heat-treated as shown in the composite FE-SEM images (Figure 7). Among these

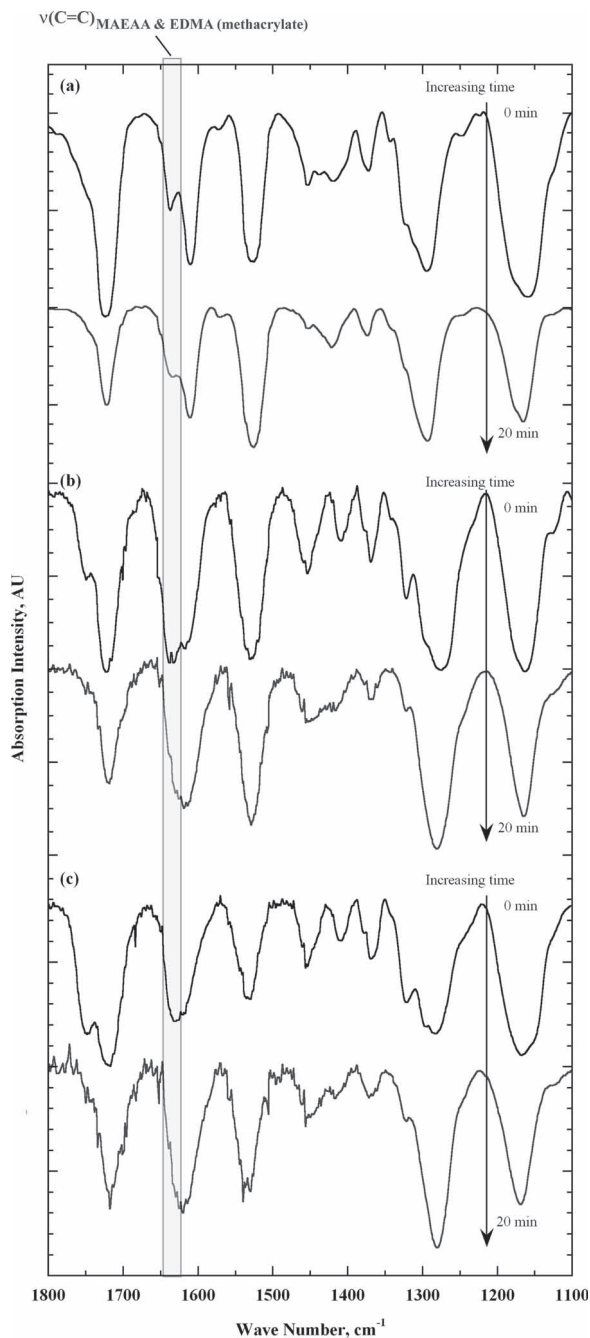


Figure 4. Time-resolved FTIR data of a) Al_2O_3 , b) TiO_2 , and c) Nb_2O_5 resists heat-treated at 120°C . Notice the peak corresponding to the polymerizable $-\text{C}=\text{CH}_2$ group decreases in intensity with increasing heat-treatment time.

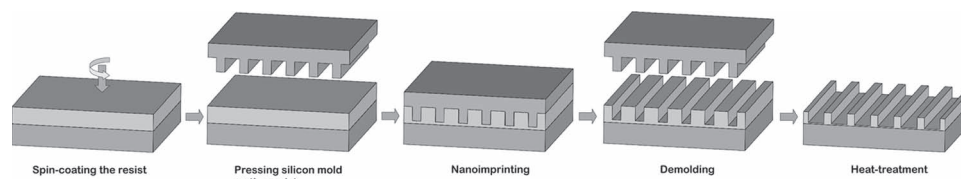


Figure 5. Schematic illustration of the nanoimprint lithography process that was used in direct patterning of oxide resists.

oxides, TiO_2 , due to its outstanding material properties, has been extensively patterned using the sol-gel route.^[9,11,15] Other oxides may also be imprinted using the sol-gel method as they form stable chelated alkoxides when reacted with β -diketones and β -ketoesters. On the other hand, only TiO_2 and ZrO_2 are amenable to NIL using the methacrylate route.^[17,18] Among the oxides imprinted in Figure 7 using the chelated monomer route, SnO_2 and GeO_2 stand out because of their unusual behavior. The former shows a very low shrinkage after heat-treatment of imprinted structures whilst the latter forms unusual residual layer pattern after imprinting. Reduction of the film thickness by diluting GeO_2 resist in *n*-butanol and subsequently imprinting it did not lead to any substantial change in the residual layer pattern. However, heat-treatment of the imprinted GeO_2 resist lead to the disappearance of this pattern. The reason for this strange behavior is unclear.

Figure 8 shows the FE-SEM images of as-imprinted and heat-treated structures of the resists containing +5 valency cations and higher. The resists in this category include Nb_2O_5 , Ta_2O_5 , V_2O_5 , and WO_3 . No attempts have been made to pattern these oxides using the sol-gel method. The methacrylate route, on the other hand, was successfully used to imprint Nb_2O_5 and Ta_2O_5 .^[18] It is interesting to note that except for WO_3 , all the imprinted structures maintain their integrity even after the heat-treatment. This characteristic behavior may be due to excessive loss of organics and/or rapid grain growth. Attempts to minimize the collapse of the imprinted structures by reducing the residual layer thickness did not yield promising results.

Direct nanoimprinting of oxides by the chelated monomer route offers significant advantages over the sol-gel and methacrylate routes. The former mainly uses a soft mold for NIL and requires a critical amount of solvent for patterning. The chelated monomer route, just like the methacrylate route, offers the convenience of liquid monomers which can be imprinted at lower pressures without worrying about the removal of solvent. It was observed that the presence of small amount of solvent left over in the spin-coated film aids in imprinting at lower pressures and its presence does not seem to hinder the free-radical polymerization. The in situ polymerization in the chelated monomer system gives rise to hardened pattern features and thus facilitates clean demolding with $\approx 100\%$ yield over $2\text{ cm} \times 1\text{ cm}$ areas. By adjusting the metal content in the overall formulation, one should be able to control the degree of pattern shrinkage after heat treatment. More importantly, unlike methacrylate route, the chelated monomer route synergistically utilizes the advantages associated with both sol-gel and methacrylate chemistries, thereby leading to an increased latitude for processing of materials. This is evidenced by the fact that our scheme is not only able to pattern oxides which

Table 3. Summary of the approximate feature size reduction at every step of the imprinting of various oxides with a 250 nm grating mold (aspect ratio = 1) using the chelated monomer route. The imprinted patterns were subjected to isothermal heat-treatment (see Supporting Information).

Resist	Feature size of the imprint after thermal polymerization		Heat-treatment conditions	Oxide feature size after the heat-treatment of imprinted structures		Total feature size reduction with respect to mold feature size [%]
	Width of imprint [nm]	Feature size reduction [%]		Width of the oxide feature [nm]	Feature size reduction [%]	
Al ₂ O ₃	225	10%	450 °C for 1 h	55	76%	78%
Ga ₂ O ₃	200	20%	450 °C for 1.5 h	43	79%	83%
In ₂ O ₃	185	26%	300 °C for 1 h	130	30%	48%
Y ₂ O ₃	165	34%	450 °C for 1 h	49	70%	80%
B ₂ O ₃	200	20%	300 °C for 3 h	150	25%	40%
TiO ₂	171	32%	450 °C for 1 h	40	77%	84%
ZrO ₂	147	41%	400 °C for 1.5 h	65	56%	74%
SnO ₂	170	32%	450 °C for 1 h	165	3%	34%
GeO ₂	162	35%	350 °C for 1 h	53	67%	79%
HfO ₂	194	22%	450 °C for 1 h	55	72%	78%
Nb ₂ O ₅	176	30%	475 °C for 1 h	57	68%	77%
Ta ₂ O ₅	197	21%	450 °C for 1 h	58	71%	77%
V ₂ O ₅	131	48%	375 °C for 1.5 h	115	12%	54%
WO ₃	175	30%	450 °C for 1 h	–	–	–

can be imprinted using sol-gel or/and methacrylate routes, but also those which are impossible to pattern with either of these two methods. Equally important is the fact that our technique, unlike step-and-flash imprint lithography,^[28] is inexpensive, fault-tolerant (with a dash of alcohol added, imprinting will still work well to give ≈100% yield) and has the potential to be extended to other types of materials as well.

A few words must be said about the long term chemical stability of the resists. Although the chelated precursors used in the preparation of the resists were found to be exceptionally stable, the same can't be said about the resists. The oxide resists for NIL were prepared by adding a cross-linker and a free-radical initiator to the corresponding chelated precursors. The presence of initiator appears to affect the long-term stability of the NIL resists. For example, Al₂O₃, Ga₂O₃, In₂O₃ and TiO₂ resists were found to be stable even after 3 months of storage. Resists for imprinting Y₂O₃, Nb₂O₅, and ZrO₂ were found to be stable for more than a month. On the other hand, V₂O₅ and WO₃ resists were stable for the time period of less than a week. Nevertheless, the chemical stability of chelated monomer-based approach is far superior to that of the methacrylate route, the latter's shelf-life ranges from anywhere between a few days to at most a month.

2.2. Limitations to Universality?

Of the variety of oxides imprinted in this study, the most egregious absence is the cations that have valencies of +1 and +2. This may suggest that our method of using chelatable monomer like MAEAA to produce precursors for NIL of oxides lacks universality. On the contrary, the problem arises primarily due to the poor solubility of alkoxides of +1 and +2 valency cations in

organic solvents. Moreover, these alkoxides can be expensive and difficult to prepare in a laboratory. The other problem which may arise is the lack of or weak chelation behavior of MAEAA with alkoxides such as those of boron and silicon. As we have seen, this problem can be circumvented by trapping their respective alkoxides in the polymer network comprising of the chelated monomer and cross-linker to produce imprinted structures.

A related issue with universality is whether monomers other than MAEAA can be used to perform NIL of oxides. Preliminary studies on imprinting of TiO₂ using allyl acetoacetate, a β-ketoester with a monomer pendent, yielded satisfactory results with ≈100% yield. It may also be surmised that β-ketoamines with a monomer group are also potential chelating agents for alkoxides to produce metal oxy-nitrides using NIL.^[29]

3. Conclusions

We have demonstrated a universal way to pattern oxides by thermal nanoimprinting lithography using stable and polymerizable precursors formed by reacting MAEAA, a chelating monomer, with alkoxides. MAEAA possesses β-ketoester and methacrylate groups—the former helps in the formation of environmentally stable, chelated alkoxide with a long shelf-life whilst the latter provides a reactive methacrylate group for in situ copolymerization with a cross-linker during imprinting. The use of MAEAA leads to synergistically utilizing the advantages of the sol-gel and methacrylate routes whilst alleviating drawbacks associated with both of them. Imprintable oxide resists were formed by mixing polymerizable chelated alkoxides with EDMA, a cross-linker, and BPO, a thermal free-radical initiator. During imprinting using a rigid silicon mold, these resists underwent thermally

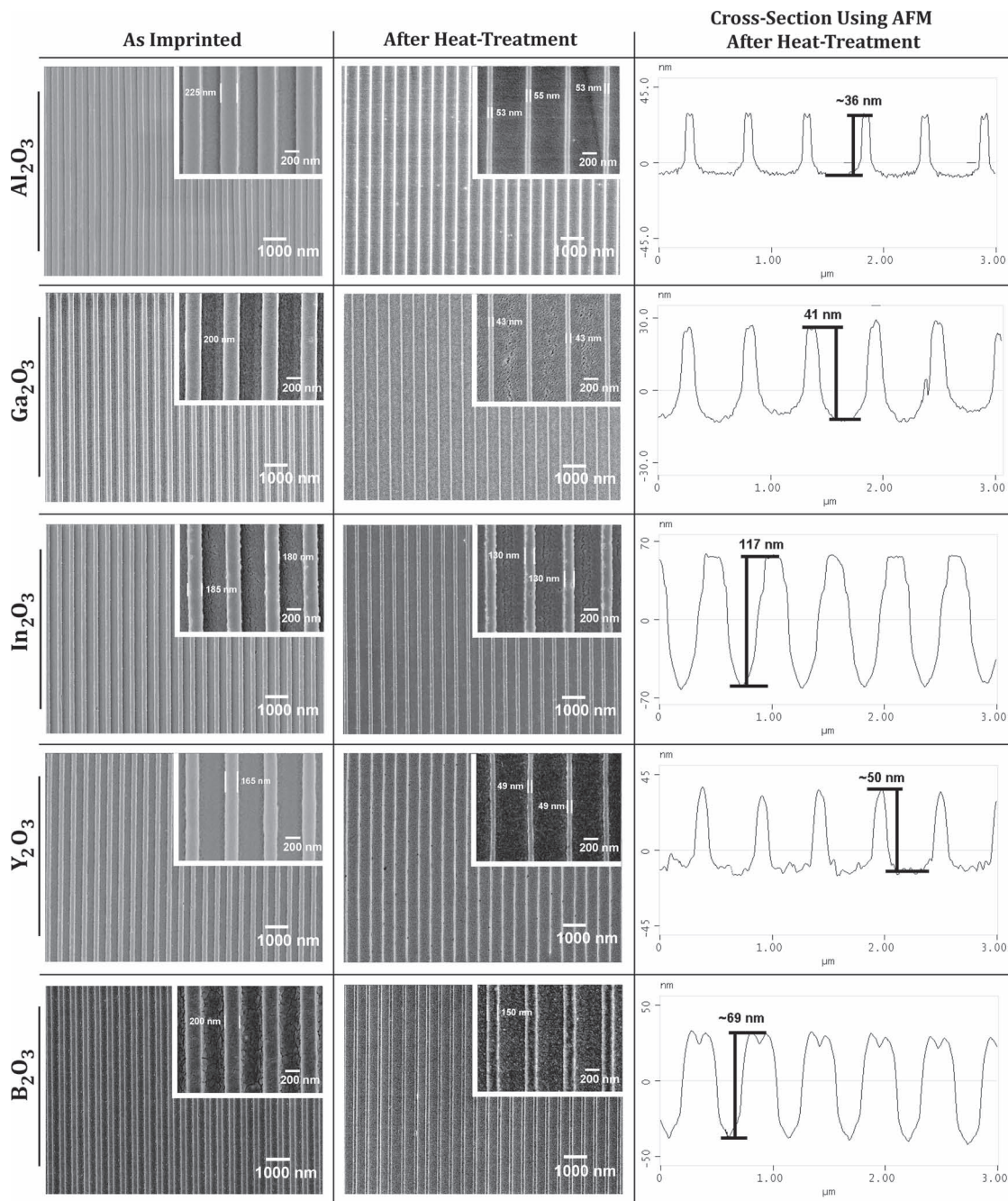


Figure 6. Imprinting of resists containing +3 valency cations. Composite FE-SEM images of as-imprinted and heat-treated structures of Al_2O_3 , Ga_2O_3 , In_2O_3 , Y_2O_3 , and B_2O_3 using a 250 nm equal line and space silicon grating mold. The insets show the structures at a higher magnification. The AFM line traces of the corresponding heat-treated imprinted structures are shown on the right.

initiated in situ free radical copolymerization that led to the trapping of the cation, lowering of surface energy of the resist and strengthening of the imprint. This enabled easy and clean demolding over $1\text{ cm} \times 2\text{ cm}$ patterned area with $\approx 100\%$ yield. Successful imprinting was demonstrated for numerous oxides such as Al_2O_3 , Ga_2O_3 , In_2O_3 , Y_2O_3 , B_2O_3 , TiO_2 , SnO_2 , ZrO_2 , GeO_2 , HfO_2 , Nb_2O_5 , Ta_2O_5 , V_2O_5 , and WO_3 . Thermolysis of the imprinted patterns yielded amorphous/crystalline oxide patterns with good integrity.

4. Experimental Section

Materials: Aluminum (III) tri-*sec*-butoxide (97%, Sigma Aldrich), tantalum (V) ethoxide (99.98%, Sigma Aldrich), tin (IV) *tert*-butoxide ($>99.99\%$, Sigma Aldrich), titanium (IV) *n*-butoxide (97%, Sigma Aldrich), vanadium (V) oxytri-*iso*-propoxide (Sigma Aldrich), niobium (V) ethoxide (99.95%, Sigma Aldrich), yttrium (III) *n*-butoxide (0.5 M in toluene, $\geq 99.9\%$, Sigma Aldrich), germanium (IV) ethoxide ($\geq 99.95\%$, Sigma Aldrich), zirconium (IV) *n*-butoxide (80 wt% solution in 1-butanol, Sigma Aldrich), hafnium (IV) *tert*-butoxide (99.9%, Alfa Aesar),

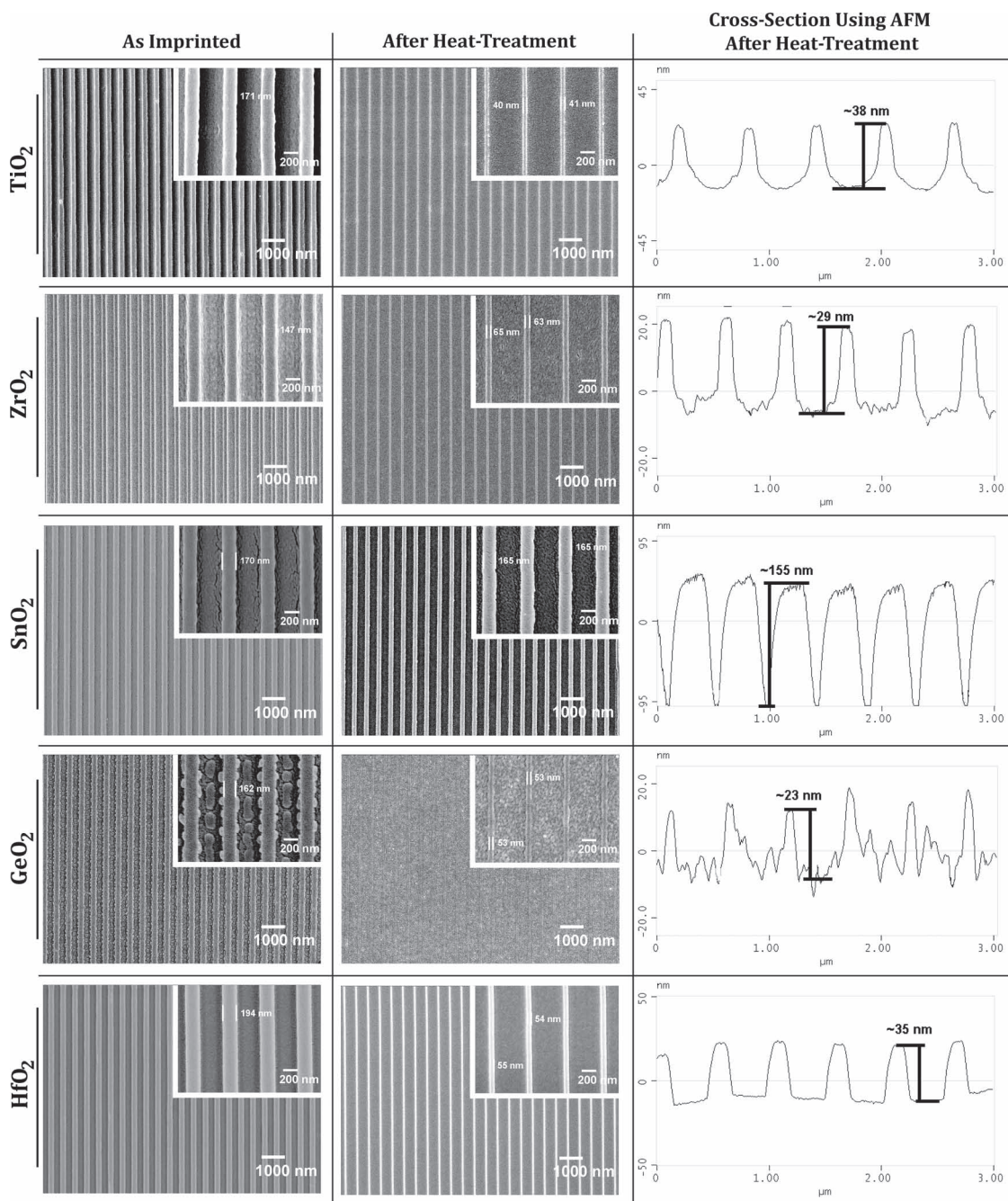


Figure 7. Imprinting of resists containing +4 valency cations. Composite FE-SEM images of as-imprinted and heat-treated line structures of TiO_2 , ZrO_2 , SnO_2 , GeO_2 , and HfO_2 using a 250 nm equal line-and-space silicon grating mold. The insets show the structures at a higher magnification. The AFM line traces of the corresponding heat-treated imprinted structures are shown on the right.

tungsten (V) ethoxide (Alfa Aesar), gallium (III) *iso*-propoxide (mixture of oligomers, 99%, Alfa Aesar), tri-*iso*-propyl borate (98%+, Lancaster Synthesis), indium *iso*-propoxide (99.9%, Multivalent Laboratory), 2-(methacryloyloxy)ethyl acetoacetate (95%, Sigma Aldrich), and 1*H*,1*H*,2*H*,2*H*-perfluorodecyltrichlorosilane (96%, Alfa Aesar) were used as received. Ethylene glycol dimethacrylate (98%) was also purchased from Sigma Aldrich and was used after removal of stabilizer using an alumina column. Benzoyl peroxide (BPO), an initiator for thermal free-radical polymerization, purchased from Sinopharm Chemical Reagent Co. Ltd., was used without any further purification.

Resists Formulation and Characterization: The alkoxides of aluminum, yttrium, boron, titanium, zirconium, tin, germanium, hafnium, tantalum, vanadium, niobium, and tungsten were reacted with MAEAA in 1:2 molar ratio inside a glove box (<5% relative humidity) to form the chelated precursor. Those alkoxides that are not in liquid form such as indium *iso*-propoxide and gallium *iso*-propoxide were first dissolved in toluene and then reacted with MAEAA in stoichiometric proportions. In all these chelation reactions, the byproduct was an alcohol that was not removed as it provided fluidity to the resist film during spin-coating. This byproduct evaporated during imprinting at temperatures >100 °C.

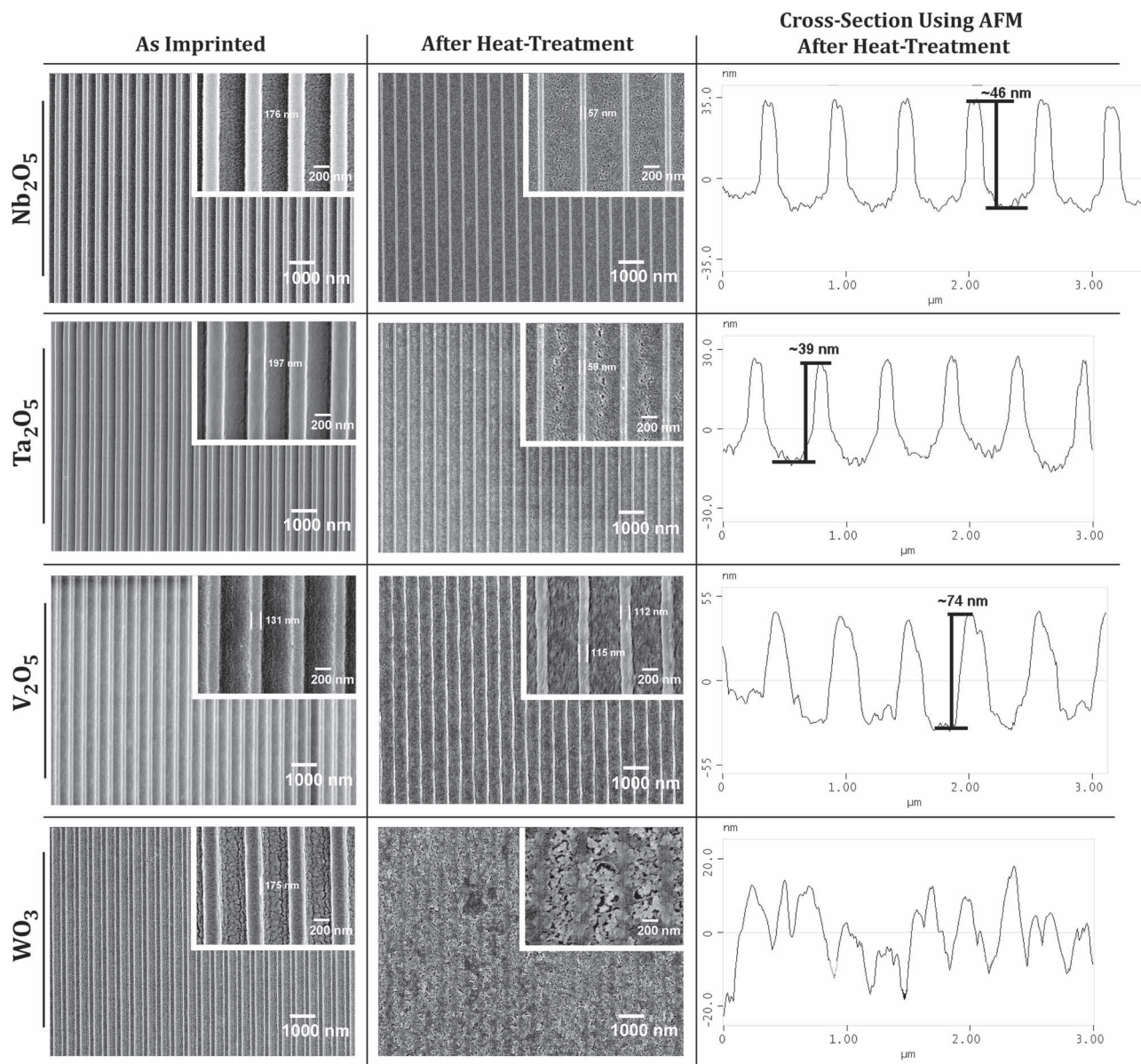


Figure 8. Imprinting of resists containing +5 valency cations and higher. Composite FE-SEM images of as-imprinted and heat-treated line structures of Nb_2O_5 , Ta_2O_5 , V_2O_5 , and WO_3 using a 250 nm equal line-and-space silicon grating mold. The insets show the structures at a higher magnification. The AFM line traces of the corresponding heat-treated imprinted structures are shown on the right.

The final resist composition for nanoimprint lithography was made by mixing the respective chelated precursors with 1.5 equivalent of the crosslinker ethylene glycol dimethacrylate (EDMA) and 2 wt% of BPO (with respect to the monomers). Hereafter, the formulations are referred to as their corresponding oxide resists. In order to study the stability of the precursors and to monitor changes in structure of the resists during polymerization, a Nicolet 6700 Fourier transform infrared (FTIR) spectroscope was used. The suitable imprinting temperatures of the resists were determined using differential scanning calorimetry (DSC, TA Instruments Q100). Thermogravimetric analysis (TGA, TA Instruments Q500) was performed to follow the degradation behavior of the resists and formation of oxides.

Nanoimprint Lithography: The silicon substrates and molds used for imprinting were cleaned with the Piranha solution (3:7 by volume of 30% H_2O_2 and H_2SO_4 . *Caution:* Extreme care must be taken while

handling the Piranha solution because it reacts aggressively with most organic materials). Before imprinting, the molds were silanized using 1H,1H,2H,2H-perfluorodecyltrichlorosilane in order to reduce the surface energy and therefore enable clean demolding after NIL. An Obducat imprinter (Obducat, Sweden) was used to carry out NIL. Suitable temperature for thermal NIL of the individual oxide resists was determined with the help of DSC measurement.

Characterization of Imprints: Scanning electron and atomic force microscopies were used to study the topography and morphology of imprinted features before and after heat-treatment. A JEOL JSM6700F field-emission scanning electron microscope (FE-SEM) was used to obtain high-resolution images of as-imprinted as well as heat-treated oxide patterns. For measuring the height of the imprinted structures, a Digital Instruments Nanoscope IV atomic force microscope (AFM) was used.

Supporting Information

Supporting Information is available from the Wiley Online Library or from the author.

Acknowledgements

The authors thank Su Hui Lim of Institute of Materials Research and Engineering (IMRE) for her assistance in performing preliminary studies. S.S.D. gratefully acknowledges the A*STAR Graduate Academy for providing him the A*STAR Graduate Scholarship for his Ph.D. study. This work was supported by the IMRE-funded core project no. IMRE/09-1C0319.

Received: September 7, 2012

Revised: October 19, 2012

Published online: November 27, 2012

-
- [1] H. Schrift, *J. Vac. Sci. Technol. B* **2008**, *26*, 458.
- [2] E. A. Costner, M. W. Lin, W.-L. Jen, C. G. Willson, *Annu. Rev. Mater. Res.* **2009**, *39*, 155.
- [3] L. J. Guo, *Adv. Mater.* **2007**, *19*, 495.
- [4] J. J. Dumond, H. Y. Low, *J. Vac. Sci. Technol. B* **2012**, *30*, 010801.
- [5] ITRS 2005 Edition, <http://www.itrs.net/Links/2005ITRS/Home2005.htm> (accessed November 2012).
- [6] M. Li, H. Tan, L. Chen, J. Wang, S. Y. Chou, *J. Vac. Sci. Technol. B* **2003**, *21*, 660.
- [7] S. J. Kwon, J. H. Park, J. G. Park, *J. Electroceram.* **2006**, *17*, 455.
- [8] O. F. Göbel, M. Nedelcu, U. Steiner, *Adv. Funct. Mater.* **2007**, *17*, 1131.
- [9] M. J. Hampton, S. S. Williams, Z. Zhou, J. Nunes, D. H. Ko, J. L. Templeton, E. T. Samulski, J. M. DeSimone, *Adv. Mater.* **2008**, *20*, 2667.
- [10] K.-Y. Yang, K.-M. Yoon, K. W. Choi, H. Lee, *Microelectron. Eng.* **2009**, *86*, 2228.
- [11] G. Shi, N. Lu, L. Gao, H. Xu, B. Yang, Y. Li, Y. Wu, L. Chi, *Langmuir* **2009**, *25*, 9639.
- [12] Y. Kang, M. Okada, K.-I. Nakamatsu, K. Kanda, Y. Haruyama, S. Matsui, *J. Vac. Sci. Technol. B* **2009**, *27*, 2805.
- [13] K.-Y. Yang, K.-M. Yoon, S. Lim, H. Lee, *J. Vac. Sci. Technol. B* **2009**, *27*, 2786.
- [14] A. Revaux, G. Dantelle, D. Decanini, F. Guillemot, A.-M. Haghiri-Gosnet, C. Weisbuch, J.-P. Boilot, T. Gacoin, H. Benisty, *Nanotechnology* **2011**, *22*, 365701.
- [15] D. A. Richmond, Q. Zhang, G. Cao, D. N. Weiss, *J. Vac. Sci. Technol. B* **2011**, *29*, 021603.
- [16] Y. N. Xia, P. D. Yang, Y. G. Sun, Y. Y. Wu, B. Mayers, B. Gates, Y. D. Yin, F. Kim, H. Q. Yan, *Adv. Mater.* **2003**, *15*, 353.
- [17] S. H. Lim, M. S. M. Saifullah, H. Hussain, W. W. Loh, H. Y. Low, *Nanotechnology* **2010**, *21*, 285303.
- [18] R. Ganesan, S. H. Lim, M. S. M. Saifullah, H. Hussain, J. X. Q. Kwok, R. L. X. Tse, H. A. P. Bo, H. Y. Low, *J. Mater. Chem.* **2011**, *21*, 4484.
- [19] R. Ganesan, S. S. Dinachali, S. H. Lim, M. S. M. Saifullah, W. T. Chong, A. H. H. Lim, J. J. Yong, E. S. Thian, C. He, H. Y. Low, *Nanotechnology* **2012**, *23*, 315304.
- [20] C. Sanchez, J. Livage, M. Henry, F. Babonneau, *J. Non-Cryst. Solids* **1988**, *100*, 65.
- [21] R. Jain, A. K. Rai, R. C. Mehrotra, *Polyhedron* **1986**, *5*, 1017.
- [22] R. Agarwal, J. P. Bell, *Polym. Eng. Sci.* **1998**, *38*, 299.
- [23] R. Lichtenberger, M. Puchberger, S. O. Baumann, U. Schubert, *J. Sol-Gel Sci. Technol.* **2009**, *50*, 130.
- [24] J. Méndez-Vivar, P. Bosch, V. H. Lara, R. Mendoza-Serna, *J. Sol-Gel Sci. Technol.* **2002**, *25*, 249.
- [25] N. Miele-Pajot, L. G. Hubert-Pfalzgraf, R. Papiernik, J. Vaissermann, R. Collier, *J. Mater. Chem.* **1999**, *9*, 3027.
- [26] M. P. Patel, M. Braden, K. W. Davy, *Biomaterials* **1987**, *8*, 53.
- [27] M. M. Haridas, J. R. Bellare, *Mater. Charact.* **1999**, *42*, 55.
- [28] R. Ganesan, J. Dumond, M. S. M. Saifullah, S. H. Lim, H. Hussain, H. Y. Low, *ACS Nano* **2012**, *6*, 1494.
- [29] D. C. Bradley, R. C. Mehrotra, D. P. Gaur, *Metal Alkoxides*, Academic Press, Orlando, FL **1978** Ch. 4.